The American Journal of Pathology, Vol. 192, No. 1, January 2022

The American Journal of
PATHOLOGY
ajp.amjpathol.org

MOLECULAR PATHOGENESIS OF GENETIC AND INHERITED DISEASES

Hepatic Steatosis in the Mouse Model of Wilson Disease Coincides with a Muted Inflammatory Response

Aline Gottlieb,* Som Dev,* Lauren DeVine,† Kathleen L. Gabrielson,‡ Robert N. Cole,† James P. Hamilton,§ and Svetlana Lutsenko*

From the Department of Physiology, the Mass Spectrometry and Proteomics Core,† the Department of Molecular and Comparative Pathobiology,‡ and the Department of Medicine,§ Johns Hopkins University School of Medicine, Baltimore, Maryland*

Accepted for publication September 15, 2021.

Address correspondence to Svetlana Lutsenko, Ph.D., Department of Physiology, Johns Hopkins University, Hunterian Bldg., Room 203, or Aline Gottlieb, M.D., Ph.D., Johns Hopkins University, Hunterian Bldg., Room 205, 725 N. Wolfe St., Baltimore, MD 21205. E-mail: lutsenko@jhmi.edu or aline.gottlieb@jhmi.edu.

Wilson disease (WND) is caused by inactivation of the copper transporter ATP7B and copper accumulation in tissues. WND presentations vary from liver steatosis to inflammation, fibrosis, and liver failure. Diets influence the liver phenotype in WND, but findings are inconsistent. To better understand the impact of excess calories on liver phenotype in WND, the study compared *C57BL/6J Atp7b*$^{-/-}$ and C57BL/6J mice fed for 12 weeks with Western diet or normal chow. Serum and liver metabolites, body fat content, liver histology, hepatic proteome, and copper content were analyzed. Wild-type and *Atp7b*$^{-/-}$ livers showed striking similarities in their responses to Western diet, most notably down-regulation of cholesterol biosynthesis, altered nuclear receptor signaling, and changes in cytoskeleton. Western diet increased body fat content and induced liver steatosis in males and females regardless of genotype; however, the effects were less pronounced in *Atp7b*$^{-/-}$ mice compared with those in the wild type mice. Although hepatic copper remained elevated in *Atp7b*$^{-/-}$ mice, liver inflammation was reduced. The diet diminished signaling by Rho GTPases, integrin, IL8, and reversed changes in cell cycle machinery and cytoskeleton. Overall, high calories decreased inflammatory response in favor of steatosis without improving markers of cell viability. Similar changes of cellular pathways during steatosis development in wild-type and *Atp7b*$^{-/-}$ mice explain histologic overlap between WND and non-alcoholic fatty liver disease despite opposite copper changes in these disorders. *(Am J Pathol 2022, 192: 146–159; https://doi.org/10.1016/j.ajpath.2021.09.010)*

Wilson disease (WND) is a disorder of copper homeostasis, caused by mutations in the ATP-driven copper transporter ATP7B.[1] For a monogenic disorder, WND presentations are unusually variable. Liver pathologies alone range from mild inflammation, pronounced steatosis, and cirrhosis, to a sudden liver failure.[2–4] Hepatic copper is always elevated in WND. However, there is no correlation between the liver copper content and specific disease manifestations with the exception of steatosis, which appears to be more pronounced when hepatic copper is higher.[5]

Recent studies have suggested that diets can impact WND manifestations. A decrease in bilirubin and copper with an increase in lymphocytes was reported in WND patients on a diet with a modified protein component.[6] In animal models of WND, feeding with high-calorie diets yielded contradictory results. In *Atp7b*$^{-/-}$ rats, a high-calorie diet (45% fat, 722 kcal/L fructose syrup, 4.5 kcal/gm total calories) worsened hepatic injury.[7] In *Atp7b*$^{-/-}$ male mice, a Western-like diet (43 kcal% carbohydrate, 41 kcal% fat, 4.7 kcal/gm total calories) triggered hepatic steatosis, but did not accelerate the disease and even somewhat improved the liver phenotype.[3] (The steatosis development in *Atp7b*$^{-/-}$ female mice has not been investigated.) Mitochondria dysfunction is seen in both *Atp7b*$^{-/-}$ mice and rats,[2,7] and therefore, it cannot fully account for this dramatic difference in liver response to excess calories.

This study was supported by the German Research Foundation grant GO 3107/1-1 (A.G.) and NIH grant RO1 90078167 (S.L.).
Disclosures: None declared.

https://doi.org/10.1016/j.ajpath.2021.09.010

The relationship between steatosis and copper is particularly puzzling. In WND patients with liver steatosis, histologic findings are indistinguishable from those of non-alcoholic fatty liver disease (NAFLD).[8,9] In fact, WND patients can be misdiagnosed with NAFLD.[9] Although experimental models of steatosis/NAFLD have been developed,[10] and the *Atp7b*-deficient animals have been characterized,[2,11–13] why steatosis in WND and NALFD are phenotypically similar is not clear. Copper misbalance has been observed in NAFLD, including non-alcoholic fatty liver (NAFL) and non-alcoholic steatohepatitis,[4,14,15] but changes in copper levels are opposite to those seen in WND. NAFLD patients have reduced intrahepatic and serum copper, and additionally show an inverse correlation between hepatic fat and copper content.[16] How copper deficit in NAFLD and copper overload in WND trigger very similar metabolic and morphologic changes in the liver is unclear. Furthermore, not all (about half) of WND patients develop liver steatosis,[17] whereas other patients have inflammation as their primary manifestation.

Nuclear receptors are known to counterbalance lipid metabolism and inflammatory response in the liver[18] and contribute to the pathogenesis of both WND and NAFLD.[19] We hypothesized that the dysregulated lipid metabolism tips the balance between steatosis and inflammation, and thus determines specific phenotypic manifestation in WND. Given that copper overload in hepatocytes is associated with down-regulation of lipid metabolism and reduced gluconeogenesis,[3,13] how calorie supplementation would modify the liver WND phenotype was tested. The results show that Western diet (WD) diminishes inflammation to favor steatosis without improving cell viability.

Materials and Methods

Animal Husbandry and Sample Collection

The originally hybrid B6; 129S1-*Atp7b*^{tm1Tcg}/LtsnkJ mice (*Atp7b*$^{-/-}$ mice) were transferred on a C57B6 background as previously described.[12] For brevity, the authors are referring to corresponding mice as *Atp7b*$^{-/-}$ knockout (ko; Wilson Disease model) mice, which the authors compared with C57BL/6J wild-type (wt) mice. Animal maintenance and experimentation followed the Johns Hopkins University Animal Care and Use Committee guidelines (protocol number M017MB385) and is reported according to the ARRIVE guidelines. At 4 weeks (±3 days) after birth, wt and ko animals were randomly assigned either to the WD (RD Western Diet, D12079B; Research Diets, New Brunswick, NJ) or normal chow (NC) group. Male and female animals ($n = 5$ per group, except ko female WD: $n = 4$) were analyzed separately. Animals were weighed weekly from 4 weeks until 10 and 16 weeks after birth. Non-fasted mice were euthanized using isoflurane, blood was collected by cardiac puncture, and livers and spleens were harvested. Blood was allowed to clot for 30 minutes in BD Microtainer tubes (Becton, Dickinson and Company, Franklin Lakes, NJ), serum was isolated by centrifugation at 4000 × *g* for 10 minutes at 4°C, and then stored at −80°C for further analysis. Measurements of metabolites were done at the Johns Hopkins University Phenocore Phenotyping and Pathology Core. A piece of liver (left lobe) was fixed with 10% formalin for sectioning and another piece with 4% paraformaldehyde for OCT compound (Tissue-Tek, Ref#-4583; Sakura Finetek, Torrance, CA) embedding the following day. The remaining tissue was flash-frozen and stored at −80°C.

Histology

Paraffin sectioning and hematoxylin and eosin staining were done at the Johns Hopkins Pathology Core. Copper in paraffin sections (7 μm) was detected using a rhodanine staining kit (Part # 9113A; Newcomer Supply, Middleton, WI). For Oil Red O staining, the OCT embedded livers were cut into 7-μm sections and mounted onto Fisherbrand Superfrost Plus Microscope slides (cat-no 12-550-15; Fisher Scientific, Waltham, MA). Sections were air-dried for 30 minutes, fixed in 10% formalin for 10 minutes, quickly dipped in 60% isopropanol, and then stained with Oil Red O solution (Sigma-Aldrich, St. Louis, MO) for 15 minutes. The slides were dipped in 60% isopropanol again, then once in deionized water, and then counterstained with Mayer's hematoxylin (Vector Laboratories, Burlingame, CA) for 3 minutes. Afterwards, slides were dipped 10 times in deionized water and mounted (Permount, Lot#-1900,186; Fisher Scientific). The images were collected using an Olympus light color microscope station (Olympus, Tokyo, Japan).

Immunofluorescence Staining

Liver sections were fixed (4% paraformaldehyde), cryosectioned (7 μm), and then stained with anti-F4/80 antibody. Images were acquired by using a LSM 800 confocal laser microscope (Zeiss, Oberkochen, Germany). TIFF files were imported into Adobe Photoshop CS6 version 13.0 (Adobe, San Jose, CA), and the entire field was enhanced and sharpened by using the levels command.

Copper Measurements

Thirty to 80 mg of tissue was digested with 200 μL of 70% nitric acid for 4 hours at 65°. When cooled to room temperature, 300 μL of Fisher Chemical HPLC-grade water (Fisher Scientific) was added, and samples were centrifuged at 2000 × *g* for 1 minute; the supernatant transferred to a 1.7-mL microtube and then stored at 4°C until the analysis. The samples were diluted with HPLC-grade water to a final concentration of nitric acid below 2% and analyzed using a PerkinElmer PinAAcle 900T Atomic Absorption Spectrometer (PerkinElmer, Waltham, MA). Copper concentrations

were calculated using standard curve and dilution factor, normalized to tissue weight, and reported as micrograms/tissue weight (in milligrams).

Protein Quantification

Thirty to 50 mg of tissue was homogenized with the hand-held battery-operated VWR pellet mixer on ice (VWR International, Radnor, PA) and incubated in lysis buffer [50 mmol/L HEPES (Sigma-Aldrich), pH 7.4, 0.1% IGEPAL (Sigma-Aldrich), 150 mmol/L NaCI (Sigma-Aldrich), 0.25 mol/L sucrose (Sigma-Aldrich), 0.5 mmol/L AEBSF (Thermo Fisher Scientific, Waltham, MA), and an EDTA-free protease inhibitor tablet (Thermo Fisher Scientific)] on ice for 20 minutes. Insoluble debris was removed by centrifugation at 700 $\times$ g for 15 minutes at 4°C. Protein concentration was determined by the BCA method.

TMT Mass Spectrometry

For mass spectrometry, 100 μg of protein per sample was used; the quality of sample and equal amounts were verified by gel electrophoresis and Colloidal Blue staining (Thermo Fisher Scientific). Proteins were reduced, alkylated, and TCA/acetone precipitated as in Aigner et al.[14] Individual samples were labeled with a unique isobaric mass tag reagent (TMT 16-plex; Thermo Fisher Scientific) according to manufacturer instructions. The tandem mass tag (TMT)-labeled peptides were analyzed by liquid chromatography interfaced with tandem mass spectrometry (LC/MSMS) using an Easy-LC 1200 HPLC system interfaced with an Orbitrap Fusion Lumos Tribrid Mass Spectrometer (Thermo Fisher Scientific). Isotopically resolved masses in precursor (MS) and fragmentation (MS/MS) spectra were processor in Proteome Discoverer software version 2.4 (Thermo Fisher Scientific). All data were searched using Mascot software version 2.6.2 (Matrixscience, Boston, MA) against the 2017_Refseq 83_mouse database. The abundances for each peptide were summed to get the protein abundances. These were normalized based on the total protein amount per channel. Analysis of variance was performed to determine the P values. Identifications from Mascot searches were filtered at 1% false discovery rate confidence threshold. Proteome Discoverer results, MSF (Magellan Storage File) research file, and complete methods can be found at Figshare (Boston, MA).

Bioinformatic Analysis

Proteome Discoverer software version 2.4 was used to generate a heatmap, principal component analysis, whiskers, and volcano plots. The associations between the altered proteins and major metabolic pathways were identified using the Ingenuity Pathways Analysis software version 01-20-04 (Ingenuity Systems; Qiagen, Germantown, MD). Differentially expressed proteins with $P < 0.05$ and a fold change of 1.5 or higher were used for the analysis.

Quantitative PCR

RNA was isolated from 20 to 50 mg of frozen liver using RNeasy Plus Mini Kit (Qiagen) and quantified using an Implen NanoPhotometer (Implen, Westlake Village, CA). Gene expression was analyzed using Power SYBR Green RNA-to-Ct 1-Step kit from Applied Biosystems (Waltham, MA) using 100 ng of RNA. Relative gene expression was analyzed on Applied Biosystems QuantStudio 6 Flex (Thermo Fisher Scientific) by the threshold cycle method with glyceraldehyde-3-phosphate dehydrogenase (GAPDH) mRNA as a reference. All primers were obtained from Integrated DNA Technologies (IDT, Coralville, IA). The primer sequences are shown in Table 1.

Triglyceride Measurements

Thirty to 40 mg of frozen liver were homogenized in 500 μL of radioimmunoprecipitation assay lysis buffer (Sigma-Aldrich) with 1× protease and phosphatase inhibitors (Roche, Basel, Switzerland), and 10 μg of sample/well were assayed in triplicate using the Infinity triglyceride (TG) assay kit (Thermo Fisher Scientific). Absorbance was measured at 540 nm using a FLUOstar Omega (BMG LabTech, Ortenberg, Germany) plate reader. The TG concentrations were calculated using a standard curve and normalized to tissue weight.

Whole-Body Composition Measurements

A whole-body Composition Analyzer (EchoMRI, Houston, TX) was used to measure mouse body composition. Scans are performed by placing the awake mouse into a thin-walled plastic cylinder (1.7-mm thick, 4.7-cm inner diameter) with a cylindrical plastic insert added to limit movement. The tube is then inserted into the instrument. The animal's hydrogen nuclei are stimulated by safe radio frequency pulses, and the system generates T1 and T2 relaxation curves specific to each

Table 1 Primers Utilized for Real-Time PCR

Primer	Sequence
FasN forward	5′-GCATTTCCACAACCCCAACC-3′
FasN reverse	5′-AACGAGTTGATGCCCACGAT-3′
GAPDH forward	5′-CACATTGGGGGTAGGAACAC-3′
GAPDH reverse	5′-AACTTTGGCATTGTGGAAGG-3′
HMG-CoA forward	5′-CCTGGGCCCCACATTCA-3′
HMG-CoA reverse	5′-CCTGGGCCCCACATTCA-3′
PPARα forward	5′-GCTGTTCTGGGTTCTCTTGG-3′
PPARα reverse	5′-TTCCATCTTCGCTGTCCTTT-3′
SCD forward	5′-GGGTGCCTTATCGCTTTCCT-3′
SCD reverse	5′-CAGCCTCTTGTCTACACCCG-3′

of the four components measured (lean, fat, free water, and total water).

Immunoblotting

Total protein lysates (25 μg in radioimmunoprecipitation assay buffer, see *Protein Quantification*) were loaded onto precast 10% SDS-PAGE gel (Bio-Rad Laboratories, Hercules, CA) and electrophoresed and transferred on the nitrocellulose membrane using a Trans-blot turbo system (Bio-Rad Laboratories). After blocking with 5% nonfat dry milk for 1 hour, membranes were incubated with primary antibodies in 1% nonfat dry milk overnight at 4°C on a shaker followed by a secondary antibody for 1 hour at room temperature. Antibodies' source and dilutions are given in Table 2.

Statistical Analysis

Statistical analysis was performed using Prism software version 8.0 (GraphPad Software, San Diego, CA). Unless otherwise stated, two-way analysis of variance was used for all the experiments. Two-tailed *t*-test was used when appropriate and mentioned specifically. All data in the figures are shown as the mean ± SD. $P < 0.05$ was considered significant.

Results

Atp7b$^{-/-}$ and wt Mice Fed Western Diet Show Similar Weight Gain but Different Adiposity

To better understand the effect of copper overload on the development of hepatic steatosis in WND, C57BL/6J (wt) and *Atp7b*$^{-/-}$ C57BL/6J (ko) mice fed with WD or NC for 12 weeks (Figure 1A and Supplemental Figure S1) were compared. At the end of the experiment (at 16 weeks after birth), the mean weight of wt males on WD (30.4 ± 6.36 g) was 9.6% higher than on NC (27.74 ± 4.99 g), and a similar trend (5.4% increase) was seen for *Atp7b*$^{-/-}$ males (28.34 ± 2.03 g on WD compared with 26.88 ± 1.33 g on NC); however, these differences were not statistically significant. Females showed no weight difference between the diets or genotypes: the wt females weighed 22.38 ± 1.56 g on NC and 23.68 ± 2.33 g on WD, and the *Atp7b*$^{-/-}$ females weighed 21.8 ± 1.73 g on NC and 22.5 ± 1.36 g on WD (Figure 1A). The weight gains over the length of the experiment were also similar for each sex regardless of the diet and genotypes (Figure 1B).

Similar weight gain on different diets was unexpected and led to the examination of the total body fat mass of the animals by nuclear magnetic resonance. Wild-type males on WD had 1.9-fold more fat compared with males on NC (21% versus 11% of body weight, respectively, $P = 0.0086$); the wt females had 1.6-fold more fat on WD than NC (19% versus 12%, respectively, $P = 0.0251$). *Atp7b*$^{-/-}$ animals had smaller increases of fat mass on WD: 1.3-fold in males (from 15% versus 11%, $P = 0.0883$) and 1.37-fold in females (from 19% versus 14%, $P = 0.3716$) (Figure 1C and Supplemental Table S1). The lower amount of adipose tissue in ko animals was also apparent upon visual examination of fad pads in the abdominopelvic cavity (Figure 1D and Supplemental Figure S1).

Atp7b$^{-/-}$ Mice Accumulate Less Triglyceride in the Liver Than C57BL/6 Mice

To further evaluate the metabolic status of animals, serum levels of cholesterol, glucose, and TG were measured. WD caused significant elevation of serum cholesterol levels in both wt and ko mice (Figure 2A, Supplemental Figure S2, and Supplemental Table S2). In agreement with previous reports, glucose levels were lower in the ko_NC animals compared with those in wt_NC[11,12] (Figure 2B). In response to WD, serum glucose was elevated in both ko and wt mice, although the statistically significant increase was observed only in the ko mice (Figure 2B, Supplemental Figure S2, and Supplemental Tables S1 and S2). WD did not change serum TGs for either genotype or sex (Figure 2C). Importantly, at the end of WD feeding, the wt and ko mice had similar levels of serum cholesterol, glucose, and TGs. Similar levels of serum metabolites, especially TGs, but different total body fat, suggested different utilization of metabolic fuels by the wt and ko tissues. Analysis of liver triglycerides supported this hypothesis. In response to WD, hepatic triglycerides were elevated in wt animals (2.6-fold in wt males, $P = 0.0140$), and 1.8-fold in females ($P = 0.0468$), and Oil Red O staining confirmed lipid accumulation (Figure 2, D and E, and Supplemental Figure S2). In the ko mice of either sex, both the biochemical measurements and the Oil Red O staining showed lower triglyceride levels compared with wt (Figure 2E and Supplemental Figure S2), indicative of reduced steatosis.

Table 2 Antibodies Used in Western Blot Analysis

	Antibody	Catalog number	Host	Dilution
Primary	FATP2 (SLC27A2)	Sino Biological, 10,145-T08	Rabbit	1:1000
Primary	ABCG8	Invitrogen, Ref# PA5-95973	Rabbit	1:1000
Primary	GAPDH	Invitrogen, Ref# PA1-987	Rabbit	1:2000
Secondary	Anti-rabbit IgG HRP-linked	Cell Signaling Technology, # 7074S	Goat	1:2000

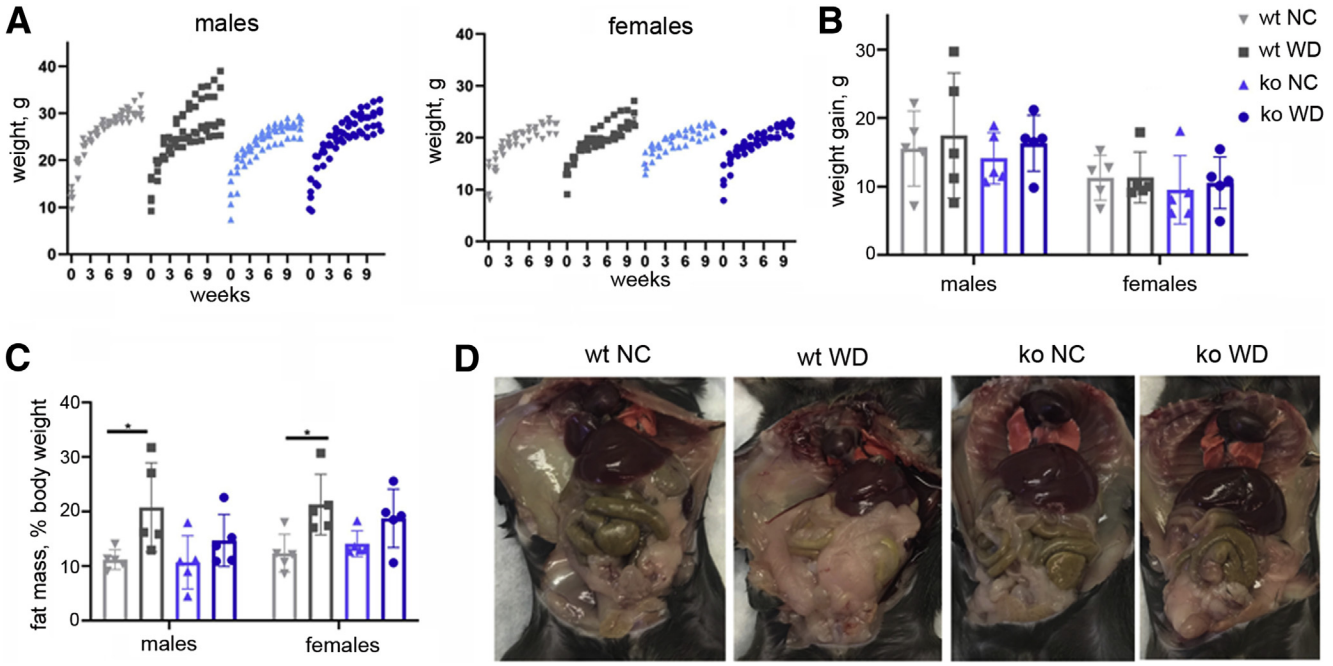

Figure 1 Effect of WD on the weight and fat mass accumulation in C57BL/6J (wt) and *Atp7b*$^{-/-}$ mice (ko). **A:** The weight changes are shown for wt (grey) and ko (blue) mice on NC (light shade) and WD (dark shade). **B:** The overall weight gain. **C:** Body fat mass. **D:** Representative images of the abdominal cavity of male mice from different feeding groups. GraphPad version 8 software was used for statistics. *$P < 0.05$ by two-way analysis of variance. ko, knockout; NC, normal chow; WD, Western diet; wt, wild-type.

Liver Proteomes Reflect Phenotypic Differences between the wt and ko Livers

To identify specific cellular and metabolic pathways associated with steatosis in wt and ko mice, liver proteomes were examined using qualitative MS. Due to high variability among the female samples, liver samples from males were selected for this analysis. The box-plot analysis confirmed that overall protein abundances and their distribution were similar in all 12 samples, and therefore, proteomes could be compared (Supplemental Figure S3). The principal component analysis plot and the heatmap showed a clear separation of samples based on the genotypes as well as the impact of WD on proteomes (Figure 3, A and B). After WD feeding, the wt and ko proteomes remained segregated, suggesting that differences in liver steatosis can be linked to differences in liver proteomes. To test this hypothesis, the WD-induced changes in wt and ko livers were characterized with respect to the respective NC controls.

Abundances of proteins known to be involved in lipid uptake and processing were evaluated first. The uptake of triglycerides into hepatocytes is facilitated primarily by CD36, FATP2, and FATP5 (Figure 3C). WD-dependent up-regulation of FATP2 and FATP5 was observed for both wt and ko; however, the abundance of these transporters in the ko liver was significantly lower compared with wt, for either diet (Figure 3D). Similar pattern—an up-regulation in response to WD in both genotypes but a lower abundance in the ko samples—was also seen for stearoyl−CoA desaturase (SCD1), which catalyzes synthesis of monounsaturated fatty acids, and for cholesterol transporter ABCG5/8. By contrast, HMG-CoA synthase, an enzyme participating in the conversion of acetyl-CoA to mevalonate, showed significant down-regulation in response to WD for both genotypes. Glucose transporter GLUT2, which supplies glucose for acetyl-CoA production, was significantly less abundant in the ko liver compared with wt liver, and was not changed in response to WD.

The MS findings were verified using quantitative PCR and Western blotting (Figure 3, E and F). The SCD1 mRNA was lower in the ko animals (males and females) and was significantly up-regulated by WD in both wt and ko, in agreement with the MS findings (Figure 3E). On Western blots, the intensity of FATP2 signal was increased by WD for both genotypes, and the ko livers had less FATP2 compared with wt on either diet, also consistent with the proteomics data (Figure 3F). As expected, lower levels of ABCG8 were observed in the ko samples compared with those in wt for both diets; however, significant increase in ABCG8 abundance was not seen in Western blots. Finally, HMGCS mRNA levels were significantly down-regulated in response to WD in both wt and ko livers, in agreement with the MS data. Taken together, these results suggest a similar response of liver to WD in both genotypes, but potentially lower uptake of lipids by the ko liver due to lower abundances of FATP2 and FATP5.

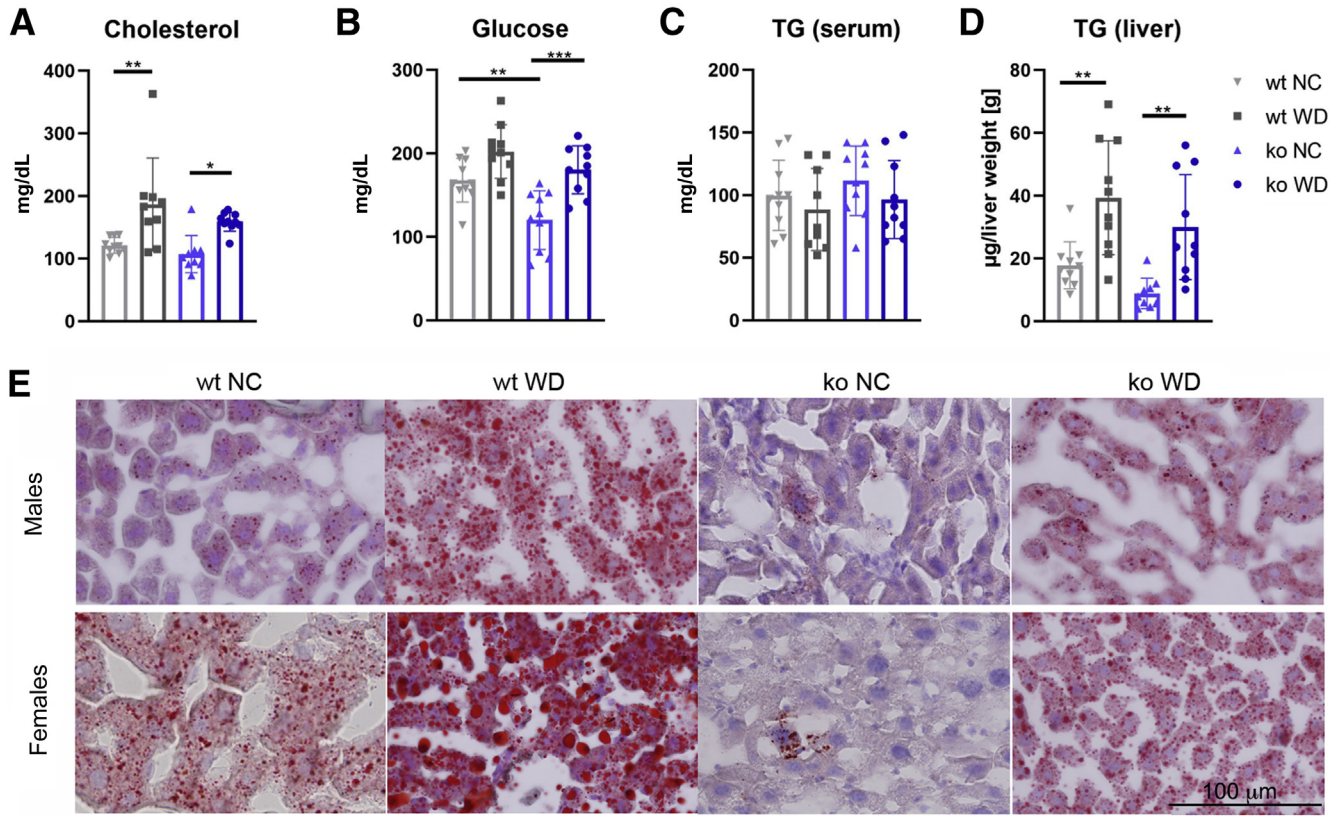

Figure 2 Wt and ko mice on WD have similar levels of serum metabolites but different fat accumulation in the liver. **A**–**C:** WD increases serum cholesterol (**A**) and glucose (**B**), whereas triglycerides (TG) remain unchanged (**C**) in both genotypes. **D:** TG levels in the liver. The levels of serum metabolites changes are shown for wt (grey) and ko (blue) mice on NC (light shade) and WD (dark shade). **E:** Oil Red O staining is noticeably reduced in *Atp7b*$^{-/-}$ on WD compared with wt; males (m), females (f). $^{**}P < 0.01$, $^{***}P < 0.001$ by two-way analysis of variance. Scale bar = 100 µm. ko, knockout; NC, normal chow; WD, Western diet; wt, wild-type.

WD Down-Regulates Cholesterol Biosynthesis and Decreases Cell Viability in the wt Liver

Ingenuity Pathway Analysis software version 01-20-04 (Thermo Fisher Scientific) was used to characterize hepatic response to WD more comprehensively. In the wt samples, the Ingenuity Pathway Analysis software identified lipid metabolism as the most impacted cellular process. The WD induced a highly significant down-regulation of cholesterol biosynthesis ($P < 10^{-24}$), which was the major metabolic pathway affected by the diet. Other changed pathways included dysregulated signaling by nuclear Retinoid-X-Receptor (RXR)–paired receptors, especially LXR/RXR, and a decreased aryl hydrocarbon receptor signaling (Figure 4A). The summary analysis of pathways, cellular processes, and upstream regulators illustrates that the WD-induced metabolic changes decrease cell viability and that the observed changes can be attributed to inhibition of such upstream regulators as SREBF2, SCAP, and RPTOR, and increased activity of POR and PEX5L. The protein abundances of SCF1 and Cyp51A1 were significantly changed by WD, likely causing their predicted lower activity (Figure 4B).

Steatosis development in the wt and ko livers is associated with similar changes in cholesterol metabolism. In the ko liver, WD induced several metabolic changes similar to those in the wt_WD liver. There were also differences (Figure 4C). WD down-regulated cholesterol biosynthesis, which was the most significantly altered metabolic pathway in the ko_WD liver ($P < 10^{-20}$), as it was in the wt_WD liver. Squalene monooxygenase, isopentenyl diphosphatase, farnesyl pyrophosphate synthase, 7-dehydrocholesterol reductase, and mevalonate kinase were significantly down-regulated in both genotypes (Table 3, Supplemental Table S3, and Supplemental Figure S4). Changes in the proteome specific to the ko liver were associated with inhibition of integrin and NRF2 signaling, diminished cell motility and cytoskeleton organization (via actin nucleation), and decreased IL-8 signaling, whereas PTEN and RhoGDI signaling was predicted to be higher (Figure 4C). These pathways were even more significantly dysregulated in the ko on NC (when compared with wt_NC) as indicated by lower *P* values, and WD mostly attenuated these changes without triggering additional ko-specific responses (Figure 5A). Finally, the predicted upstream regulators in the ko_WD also showed partial overlap with the regulatory factors in the wt_WD liver: the regulators of cholesterol biosynthesis SREBF2 and SCAP were inhibited, whereas cytochrome P450 oxidoreductase POR and peroxisomal receptor PEX5L were activated. In the ko liver, WD also affected oxidative-stress

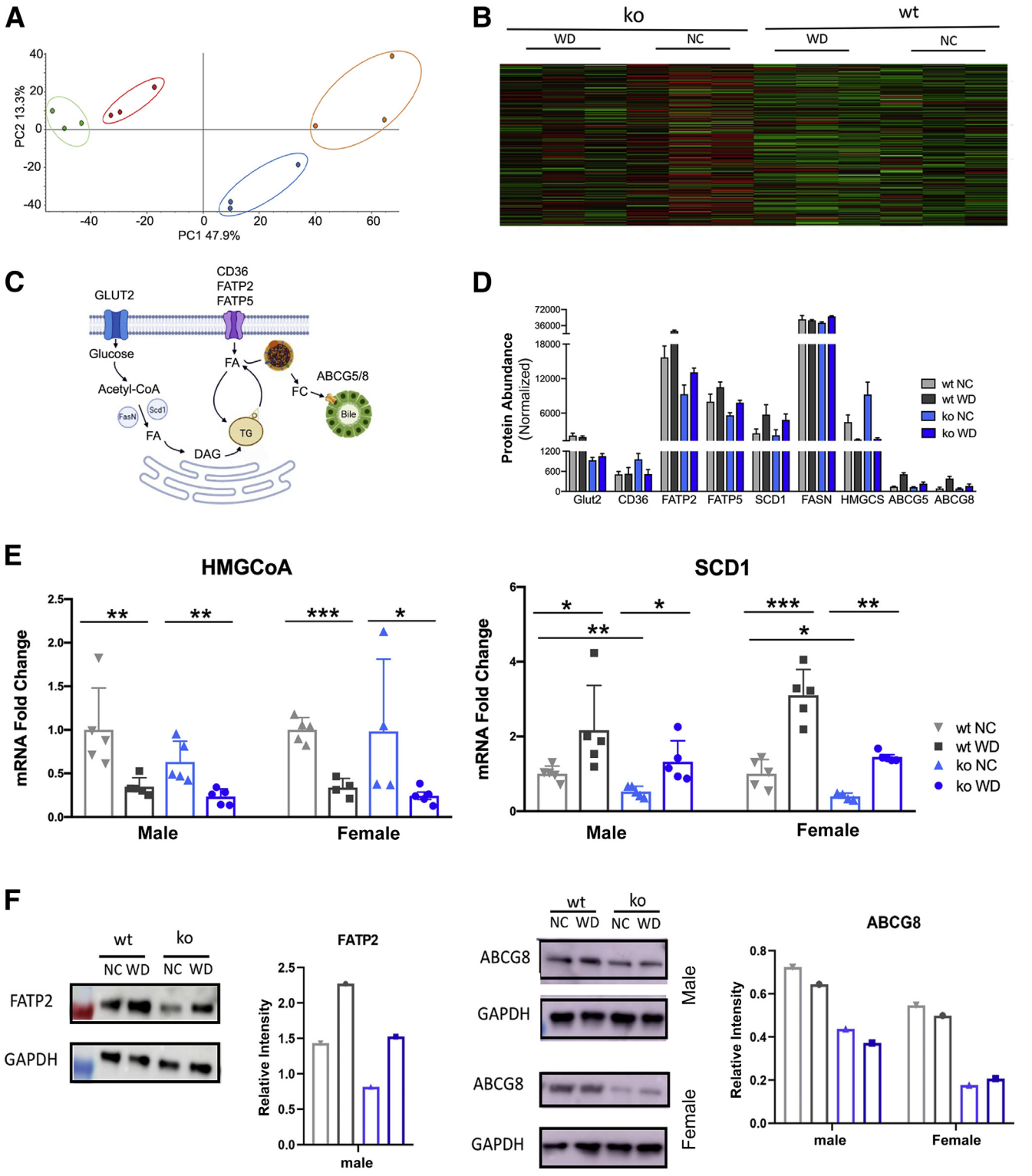

Figure 3 Quantitative analysis of WD-induced changes in liver proteome in wt and ko male mice. **A:** Principal component analysis of different feeding groups (wt_NC data are in green, wt_WD is red, ko_NC is orange, and ko_WD is blue). **B**: The heatmap showing protein profiles within the four feeding groups. From **left** to **right**: ko WD, ko NC, wt WD, wt NC. (Proteome Discoverer software version 2.4). **C** and **D:** A simplified cartoon illustrating main pathways involved in hepatic fat processing (**C**) and abundances of these proteins in male livers as determined by tandem mass tag—labeling mass spectrometry (**D**). Wt (grey) and ko (blue) mice on NC (light shade) and on WD (dark shade). **E:** The mRNA levels for HMG-CoA reductase and SCD1 as determined by quantitative PCR. **F:** Western blot and quantitation for FATP2 (left) and ABCG8 (right). The changes in liver proteome are shown for wt (grey) and ko (blue) mice on NC (light shade) and WD (dark shade). GraphPad version 8 software was used for statistics. $n = 3$ per group (**B**). $^{*}P < 0.05$, $^{**}P < 0.01$, and $^{***}P < 0.001$ by two-way analysis of variance. ABCG5/8, ATP-binding cassette sub-family G member 5/8; CD36, cluster of differentiation 36; DAG, diacylglycerol; FA, fatty acid; FasN, fatty acid synthase; FATP2 and FATP5, fatty acid transport protein 2 and 5; FC, free cholesterol; ko, knockout; NC, normal chow; SCD1, stearoyl-CoA desaturase-1; TG, triglycerides; WD, Western diet; wt, wild-type.

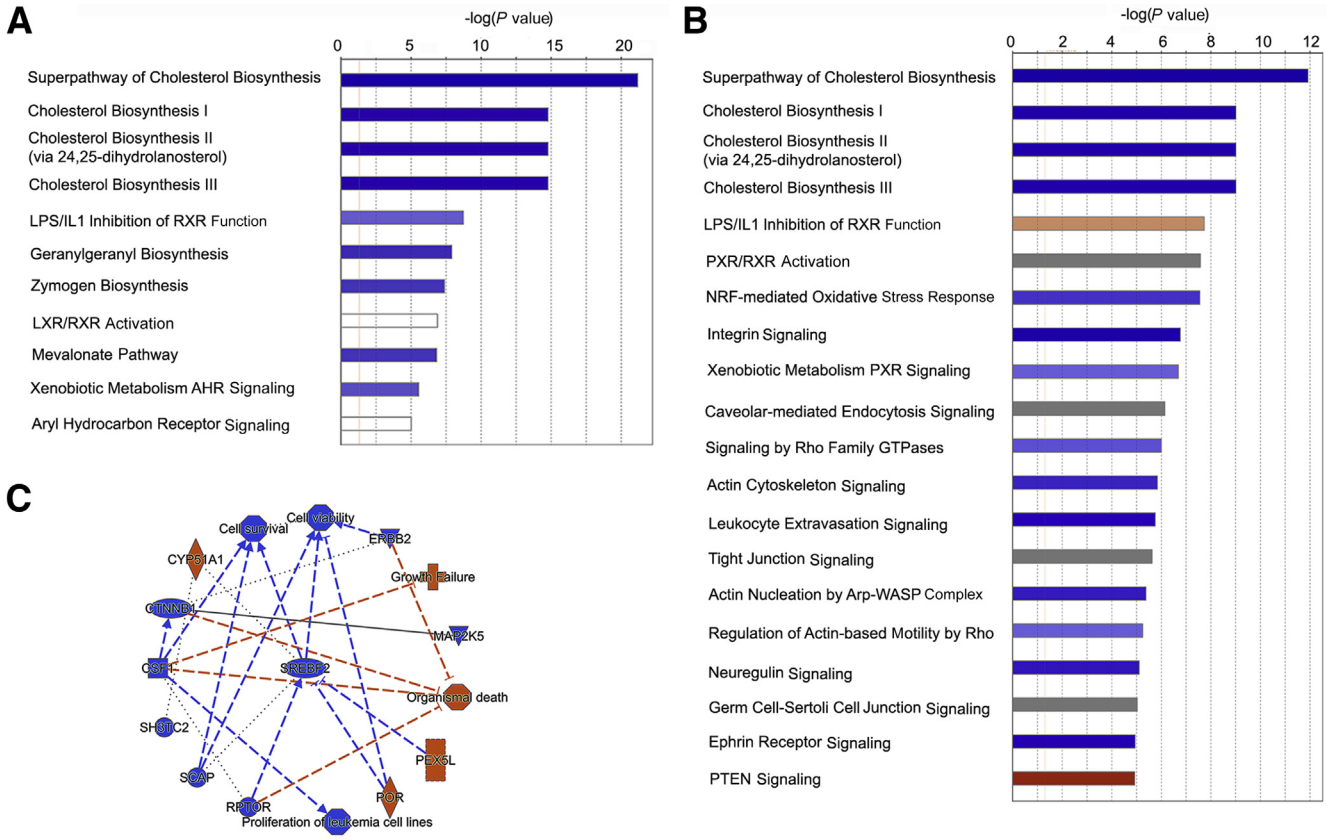

Figure 4 Similarities and differences between the wt and ko liver response to WD identified by IPA. **A** and **B**: The most significantly changed (*P* value $<10^{-5}$) metabolic and signaling pathways in the wt_WD liver compared with wt_NC (**A**) and in the ko_WD liver compared with ko_NC (**B**). In each panel, the blue indicates down-regulation/inhibition; orange, activation/up-regulation; and white or grey, dysregulation in no particular direction. **C:** Major predicted upstream regulators and biological processes affected by WD in the wt liver. ko, knockout; NC, normal chow; WD, Western diet; wt, wild-type.

response regulator NRF2, cytokine IL4, EGF, neuregulin, and FOXM, all of which were predicted to be inhibited. SPDEF activity was predicted to be increased (Figure 5B).

WD Partially Decreases Copper Content of KO Livers

The larger number of affected pathways and regulators in the ko_WD liver compared with wt_WD was likely a reflection of an abnormal metabolic status of the ko liver caused by copper overload. WD somewhat diminished the signaling by an oxidative stress response factor NRF2 (the *P* value increased from 1×10^{-12} to $1 \times 10^{-7.6}$, but remained highly significant) (Figure 5A). Consequently, whether WD lowered copper levels in the liver was examined. The hepatic copper content was characterized using histologic staining and atomic absorption spectrometry. Rhodanine signal was strong in ko_NC livers in agreement with their high copper content (Figure 6A). In ko males, WD reduced the rhodanine signal (Figure 6A), suggesting that WD decreased hepatic copper. Absorption spectrometry measurements confirmed a reduction of hepatic copper in ko_WD males in comparison to ko_NC (Figure 6B and Supplemental Table S4). Nevertheless, copper remained high when compared with the wt liver. WD did not affect hepatic copper content in females. WD also triggered 75% reduction in copper levels in spleen of ko females, but not males (Figure 6C). Adipose tissue showed no significant changes in the copper content for either genotype or feeding group (Figure 6D).

WD Blunts the Consequences of Atp7b Inactivation in Mice

Despite persistent copper elevation in the ko liver, WD appears to lessen the impact of high copper on liver proteome. When the ko_NC and ko_WD proteomes were compared with the common denominator wt_NC proteome, almost every signaling pathway in the ko_WD liver showed lower Z-score values than in the ko_NC liver (Figure 7A). For example, integrin, RhoGDI, and actin cytoskeleton signaling were all less activated in the ko_WD liver than in the ko_NC liver (Figure 7A). The WD-dependent effect on signaling pathways was associated with both the lower number of affected proteins as well as smaller fold change (Figure 7B). Similarly, comparison of proteins most significantly changed in the ko_NC and ko_WD proteomes (each plotted against wt_NC), showed fewer changes in ko_WD mice than in ko_NC mice (Figure 7C). In particular, cytochrome P450 enzymes that carry out many detoxification functions[20,21] and glutathione S-transferases were less significantly changed in ko_WD samples. The fold change

Table 3 Changes in Enzymes Associated with Cholesterol Biosynthesis

Symbol	Protein name	wt WD/wt NC	ko WD/ko NC
CYP51A1	Cytochrome P450 family 51 subfamily A1	−5.051	−4.785
DHCR24	24-Dehydrocholesterol reductase	−1.842	−2.212
DHCR7	7-Dehydrocholesterol reductase	−2.660	−1.988
FDFT1	Farnesyl-diphosphate farnesyltransferase 1	−2.041	−1.727
FDPS	Farnesyl diphosphate synthase	−7.092	−4.274
HMGCR	3-Hydroxy-3-methylglutaryl-CoA reductase	−1.681	−2.000
HMGCS1	3-Hydroxy-3-methylglutaryl-CoA synthase 1	−2.833	−6.711
HSD17B7	Hydroxysteroid 17-beta dehydrogenase 7	−2.294	−1.880
LSS	Lanosterol synthase	−2.273	−2.288
MSMO1	Methylsterol monooxygenase 1	−4.717	−5.102
MVD	Mevalonate disphosphate decarboxylase	−3.846	−3.247
MVK	Mevalonate kinase	−4.016	−2.967
NSDHL	NAD(P) dependent steroid dehydrogenase-like	−4.785	−3.460
PMVK	Phosphomevalonate kinase	−2.577	−1.894
SQLE	Squalene epoxidase	−6.061	−4.292
TM7SF2	Transmembrane 7 superfamily member 2	−2.008	−1.546

Abbreviated cholesterol biosynthesis pathway (enzymes are in parentheses): acetoacetyl-CoA/acetyl-CoA → HMG-CoA→ mevalonate (MVK)→isopentenyl-pyrophosphate (IPP, FDPS) → squalene (SQLE/LSS) → lanosterol → cholesterol (for complete list see Supplemental Figure S4).
ko, knockout; NC, normal chow; WD, Western diet; wt, wild-type.

in the abundance of proteins associated with signaling by neutrophil chemotactic factor IL-8, regulation of cytoskeleton (stathmin) and immune response (interferon-α regulator protein) was also reduced by WD (Figure 7, B and C, and Supplemental Table S5). Metallothioneins MT1 and MT2 remained highly elevated in agreement with high copper values in both ko_NC and ko_WD livers. As predicted by other data, cholesterol biosynthesis was more significantly affected in ko_WD than in ko_NC livers.

Steatosis Development in the ko Mice Coincides with a Muted Inflammatory Response

The WD-dependent inhibition of many signaling pathways in the ko liver suggested that the pathologic changes observed in ko_NC, such as inflammation, can be reduced by WD. To test this hypothesis, liver inflammation was characterized in more detail. Hematoxylin and eosin staining of wt_WD liver sections illustrated development of macrosteatosis without lobular inflammation (Figure 8A and Supplemental Figure S5). The ko_NC samples showed typical features of WND such as anisocytosis, massive lobular inflammation, and presence of polynuclear cells. The ko_WD livers showed macrosteatosis that was reduced by 30% compared with that in wt_WD livers. Additionally, the cell architecture appeared more organized, and anisocytosis as well as lobular inflammation was significantly reduced compared with ko_NC, as evident from the inflammatory scoring of either ko_WD male ($P = 0.0003$) or female ($P = 0.0165$) samples (Figure 8B). Evaluation of

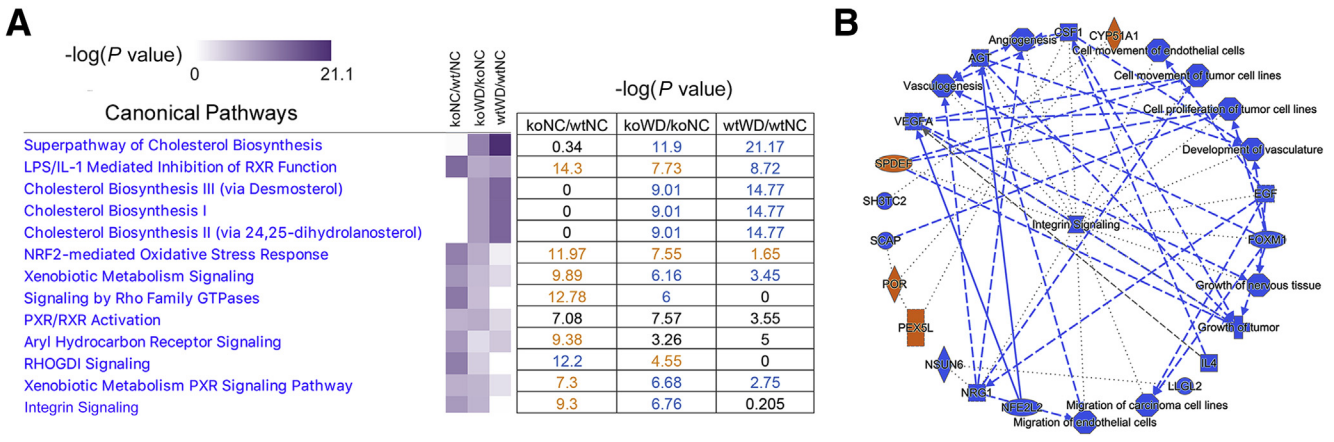

Figure 5 WD modulates changes in the metabolic and signaling pathways in the ko liver. **A:** The heatmap (left) and the corresponding *P* values (right) compare changes in canonical pathways for the wt and ko livers in response to WD, as well as changes in the ko_NC liver compared with wt_NC. Darker purple color in a heatmap illustrates more significant changes (lower *P* value); the colors in the table indicate whether the pathway is inhibited (blue), activated (orange), or dysregulated in no particular direction (black). **B:** Major predicted upstream regulators and biological processes affected by WD in the ko liver. ko, knockout; NC, normal chow; WD, Western diet; wt, wild-type.

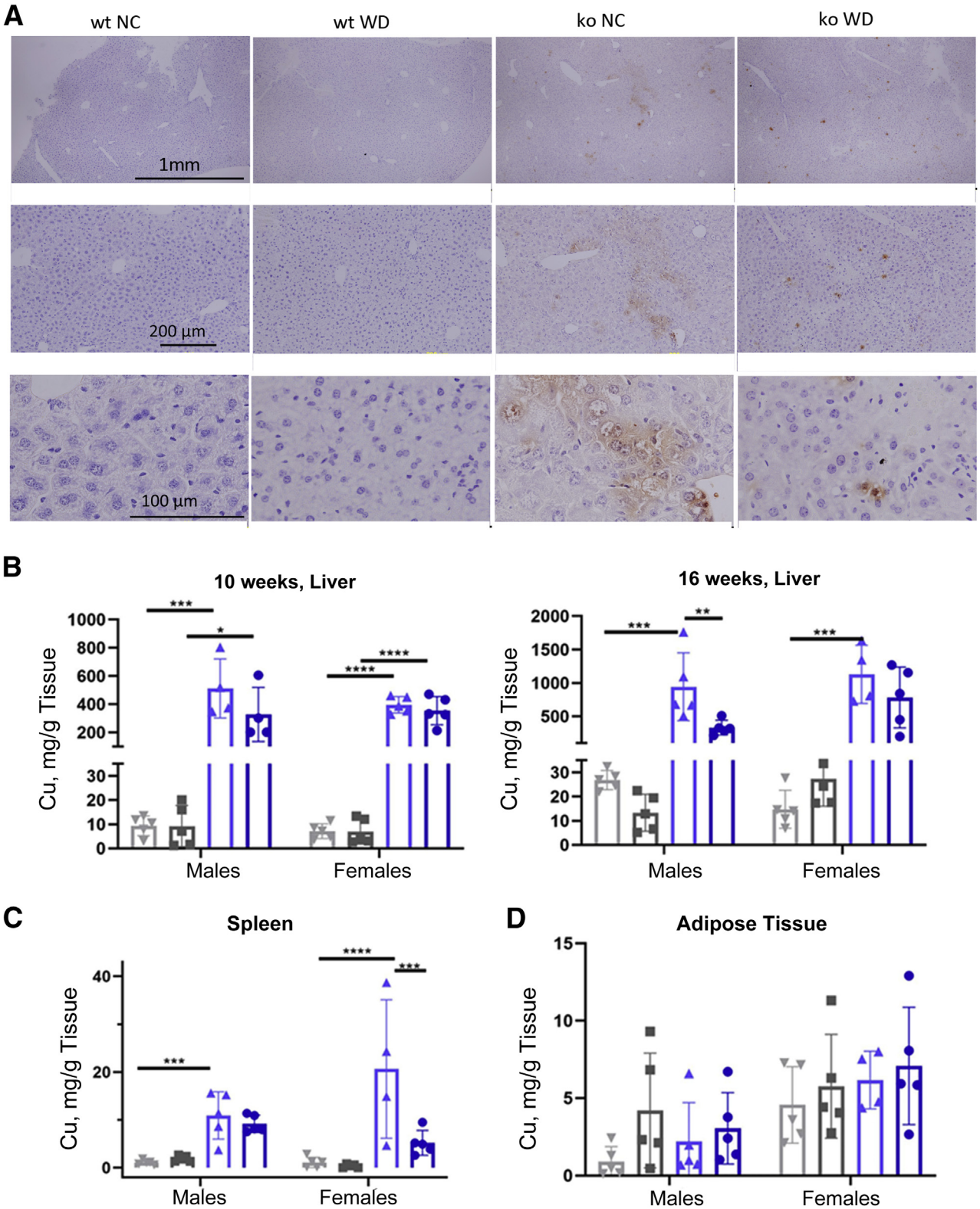

Figure 6 Changes in the tissue copper content in response to WD. **A:** Representative rhodanine staining of liver tissues (female mice). There is no rhodamine signal in the wt groups regardless of the diet, but a noticeable decrease of rhodanine staining in ko_WD animals compared with ko_NC animals. **B:** Copper levels, at 10 weeks, are significantly elevated in ko animals regardless of diet. Copper levels in wt mice do not differ between the feeding groups or the sex. Copper levels in ko mice are lower compared with NC at that age. At 16 weeks, copper changes occur in both genotypes due to WD. In wt males, hepatic copper decreases in response to WD, whereas it increases in wt females. *Atp7b*$^{-/-}$ males on WD show significantly reduced copper levels compared with ko_NC males. **C:** Spleen copper levels are significantly reduced in ko females ($P = 0.0004$), but not in ko males on WD compared with ko_NC ($P = 0.9448$). **D:** There are no changes of copper content in adipose tissue. The changes the tissue copper content are shown for wt (grey) and ko (blue) mice on NC (light shade) and WD (dark shade). GraphPad version 8 software was used for statistics. . *$P < 0.05$, **$P < 0.01$, ***$P < 0.001$, and ****$P < 0.0001$ by two-way analysis of variance. Scale bars: 1 mm (**A, top row**); 200 µm (**A, middle row**); 100 µm (**A, bottom row**). ko, knockout; NC, normal chow; WD, Western diet; wt, wild-type.

A

Signaling Pathways	Z-score	ko_NC	ko_WD
Signaling by Rho Family GTPases		4.459	1.633
Hepatic Fibrosis Signaling Pathway		4.426	1
Actin Cytoskeleton Signaling		4.041	1.342
RHOGDI Signaling		-3.9	-1.342
Ephrin Receptor Signaling		4	-1
Thrombin Signaling		3.578	1.342
Endothelin-1 Signaling		3	1.342
Integrin Signaling		4.158	N/A
Nicotine Degradation II		-2.138	-1.897
PTEN Signaling		-2.673	1.342
RAC Signaling		3.9	N/A
Adrenomedullin Signaling Pathway		2.84	1
PAK Signaling		2.84	1
Nicotine Degradation III		-1.941	-1.897
IL-8 Signaling		3.8	0
D-myo-inositol-5-phosphate Metabolism		3.771	N/A
CXCR4 Signaling		3.771	N/A
Stearate Biosynthesis I (Animals)		-1.414	-2.236
Superpathway of Inositol Phosphate Compounds		3.578	N/A
Estrogen Receptor Signaling		2.746	0.816
Sirtuin Signaling Pathway		1.279	2.236
mTOR Signaling		2.5	1
Fcγ Receptor-mediated Phagocytosis in Macrophages :		3.464	N/A
3-phosphoinositide Biosynthesis		3.441	N/A

B

PROTEIN ID	PROTEIN NAME	ko NC	ko_WD
Signaling by Rho GTPases		**41**	**5**
ARFGEF16	ADP Ribosylation Factor GEF2	3.7	2.4
ARGEF5	Rho Guanine Exchange Factor 5	2.1	1.7
RAC1	Rac Family Small GTPase 1	1.5	nc
ROCK2	Rho Associated coil-coil Containing Protein Kinase	1.9	nc
STMN1	Stathmin	8.2	nc
Actin Cytoskeleton Signaling		**27**	**4**
MYL12B	Myosin Light Chain 12B	3.1	2.1
MYH9	Myosin Heavy Chain 9	1.5	nc
WAS	WASP Actin Nucleation Promoting Factor	1.6	nc
SHC1	SHC Adaptor Protein 1	1.8	1.6
CFL1	Cofilin	1.5	nc
Integrin Signaling		**31**	**2**
ITGB1	Integrin Subunit Beta 1	1.5	nc
ITGB2	Integrin Subunit Beta 2	2.1	nc
PLCgamma2	Phospholipase C Gamma 2	2.1	nc
ARFGEF7	ADP Ribosylation Factor GEF7	1.6	n/c
IL-8 Signaling		**30**	**3**
EGFR	Epidermal Growth Factor Receptor	-2.8	-1.98
SRC	SRC Tyrosine Kinase	3.2	n/c
CSTB	Cystatin B	2.1	n/c
Cholesterol Biosynthesis		**3**	**16**
FDPS	Farnesyl-diphosphate Synthase	-1.8	-7.7
HMGCS1	3-hydroxy-3-methylglutaryl-CoA Synthase	2.4	-2.8
MSMO1	Methylsterol Monooxygenase1	nc	-5.3

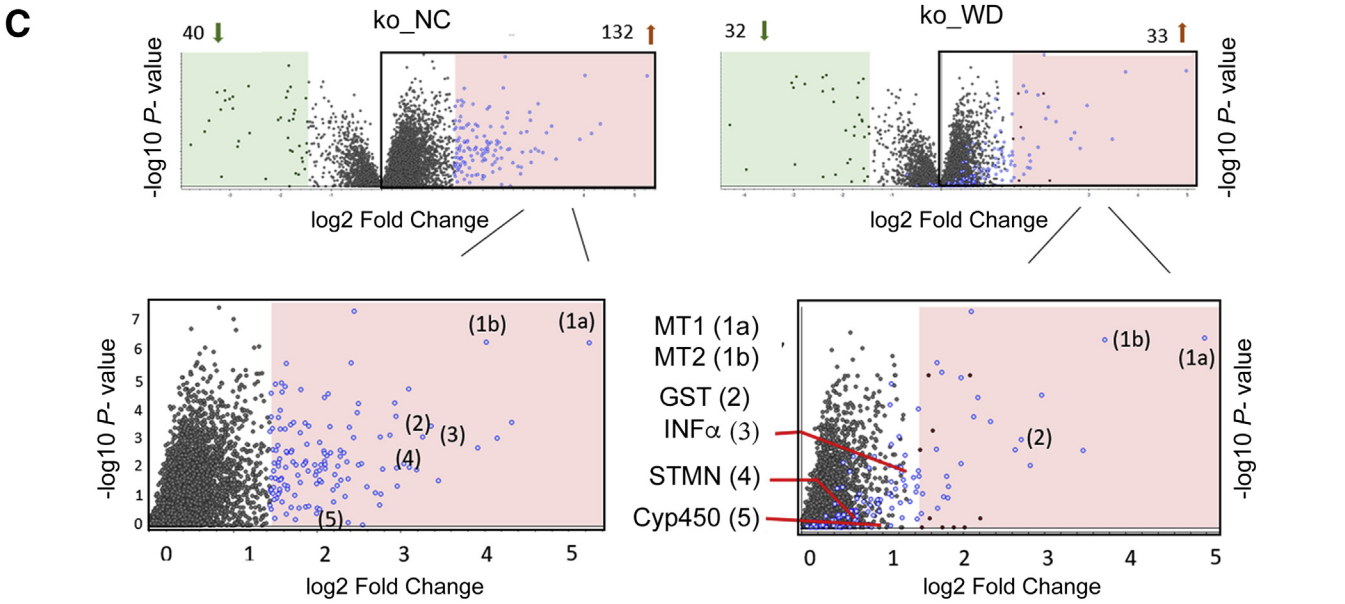

Figure 7 WD mutes the signaling pathways and ameliorates changes in protein expression in *Atp7b*$^{-/-}$ mice. **A:** The heatmap and Z-score values illustrate the status of signaling pathways in ko_NC and ko_WD when their proteomes are compared with normal wt mice. Orange indicates activation; blue, inhibition. **B:** Examples of pathways and associated proteins changed in response to WD. Each genotype is compared with wt_NC. Numbers in bold indicate the number of altered proteins within the respective pathway. Created with Ingenuity Pathway Analysis software version 01-20-04. **C:** The volcano plot for ko_NC (40 down- and 132 up-regulated proteins) and ko_WD mice (32 down- and 33 up-regulated proteins) when compared with wt_NC. **Pink and green panels** indicate changes larger than |log2| = 1.3. **Bottom panels** show an enlarged area the corresponding **top panel** with up-regulated proteins (highlighted in blue) illustrating how several of them change in response to WD. Created with Proteome Discoverer software version 2.4. Cyt P450, cytochrome P450 family; GST, glutathione S-transferase; INFα, interferon alpha regulatory protein; ko, knockout; MT1 and 2, metallothionein 1 and 2; , N/A, no change; NC, normal chow; STMN1, stathmin; WD, Western diet; wt, wild-type.

inflammatory markers in the mouse livers further confirmed reduced inflammatory response. CD24a levels were significantly lower in *Atp7b*$^{-/-}$ males ($P = 0.0026$) and females ($P = 0.003$) fed the WD (Figure 8C). TNFα levels (Figure 8D) were significantly reduced in female mice ($P = 0.0012$), but not changed in males ($P = 0.984$). Inducible nitric oxide synthase (iNOS) levels (Figure 8E) are significantly elevated in ko mice on NC, but not in ko mice on WD, whereas IL1β levels did not show any significant changes among the genotypes and feeding groups (the authors' data, not shown). F4/80 staining of liver sections revealed no noticeable changes between genotypes and feeding groups (Supplemental Figure S6), suggesting that inflammation is driven more by leukocytes rather than macrophages. Taken together, these results demonstrate that in *Atp7b*$^{-/-}$ mice, the onset of diet-induced macrosteatosis coincides with a decreased inflammatory response.

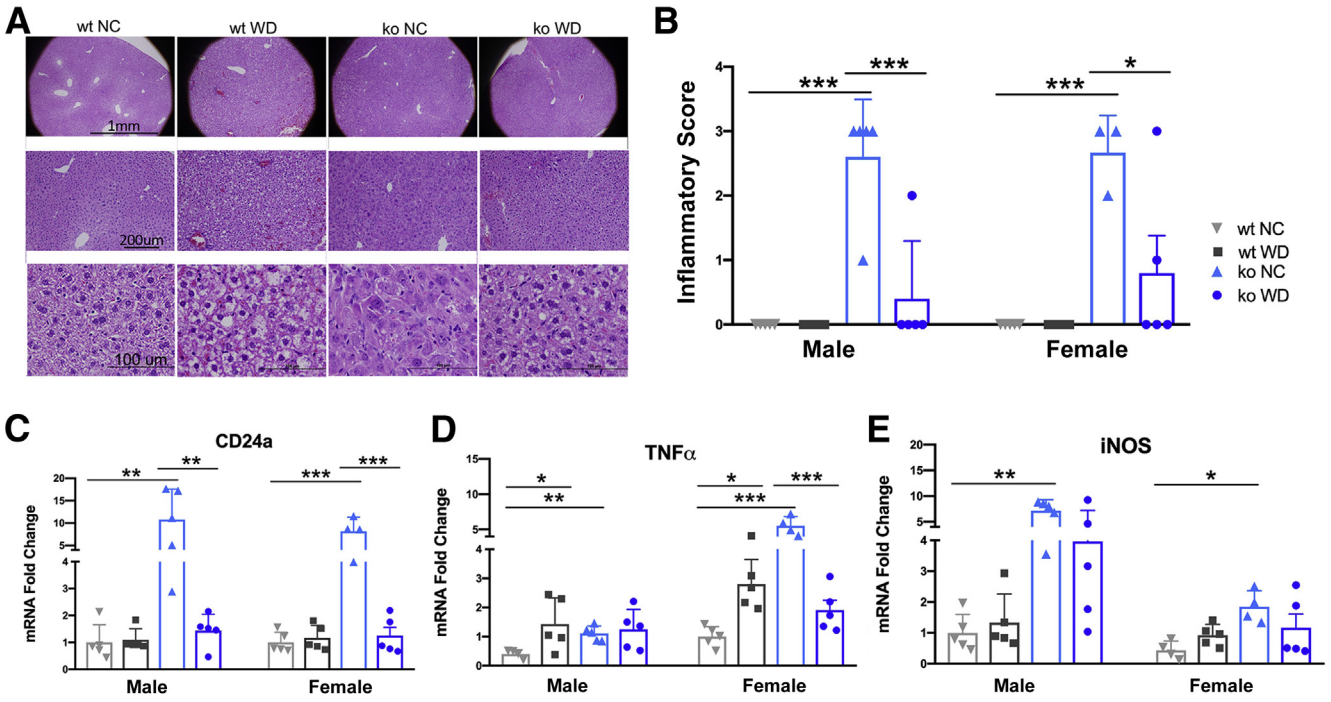

Figure 8 WD improves liver histology in *Atp7b*$^{-/-}$ mice and decreases inflammatory markers. **A:** Hematoxylin and eosin (H&E) staining of female mice show improvement of liver histology in ko animals on WD. **B:** Inflammatory scoring performed by a pathologist (0, no inflammation; 1, minimal; 2, mild; 3, moderate; 4, severe, which did not occur). **C**–**E:** Quantitative PCR data showing reduction in CD24a (**C**), INFα (**D**), and iNOS levels (**E**). The changes are shown for wt (grey) and ko (blue) mice on NC (light shade) and WD (dark shade). GraphPad version 8 software was used for statistics. . $^{*}P < 0.05$, $^{**}P < 0.01$, and $^{***}P < 0.001$ by two-way analysis of variance. Scale bars: 1 mm (**A, top row**); 200 μm (**A, middle row**); 100 μm (**A, bottom row**). ko, knockout; NC, normal chow; WD, Western diet; wt, wild-type.

Discussion

Here, the study shows that diets could be a significant attenuating factor in WND liver phenotype. Steatosis develops similarly in C57BL/6J (wt) and *Atp7b*$^{-/-}$ (ko) mice, and inhibition of cholesterol biosynthesis is the major metabolic change associated with the onset of steatosis in both cases. Significantly, cholesterol biosynthesis is already inhibited in *Atp7b*$^{-/-}$ mice at 6 weeks after birth,[2] but ko liver TGs are low, and without WD, steatosis does not develop (this study and Wooton-Kee et al[3]). These results confirm the view that down-regulation of cholesterol metabolism is a metabolic adjustment rather than a cause of hepatic fat accumulation.[22,23]

WD accelerates liver disease and worsens the phenotype in a WND rat model.[7] However, in that study, the chosen time point to start feeding the rats was significantly later (age 6 to 8 weeks compared with 4 weeks in this study), when rats already showed compromised liver function, and the given WD contained 45%kcal from fat and fructose syrup in drinking water, which contains more fat and calories per day as a standardized WD in humans. By contrast, liver disease does not worsen in *Atp7b*$^{-/-}$ mice, where histology, changes in proteome, and liver function are improved. We speculate that in addition to the aforementioned differences in conducting the studies, an increased up-regulation of metallothioneins in mice compared with rats results in more efficient copper sequestration and less copper-mediated oxidative stress and mitochondrial toxicity.[3] In addition, in mice, copper remains high and alterations of the cellular pathways associated with cell survival predict increased mortality; therefore, the positive effects of WD are likely to be transient.

Inhibition of nuclear receptors LXR, RXRα, and PPARa along with changes in lipid metabolism and bile acid production are common for NAFLD and are also identified in WND.[24] Nuclear receptor activation improves the liver phenotype of *Atp7b*$^{-/-}$ mice[19] and could contribute to WD-induced improvement seen in this study. Indeed, both mouse strains on WD show proteome changes that indicate increased activity of nuclear receptors such as LXR/RXR and dysregulation of FXR/RXR targets (Z-score 2.4). However, in both strains, the targets of other regulators such as RPTOR are even more altered (Z-score < -4). Which of these regulators play a primary role in the onset of steatosis and how they work together needs to be tested in the future.

Integrin signaling and inflammatory response are up-regulated in *Atp7b*$^{-/-}$ mice, and WD mutes these responses.

Integrin signaling enhances leukocyte trafficking and helps to maintain hepatic transcriptional and metabolic programs that sustain oxidative metabolism and glucose homeostasis.[25–27] Data from the current study suggest that WD inhibits cell motility and also increases availability of metabolic fuels by up-regulating expression of fatty acid transporters. *Atp7b*$^{-/-}$ livers are deficient in metabolic fuels (TGs and glucose). Higher availability of TGs may improve the metabolic status of *Atp7b*$^{-/-}$ liver.

It is interesting that whereas cytosolic HMG-CoA synthase is down-regulated by WD in both genotypes (decreasing cholesterol production), the mitochondrial HMG-CoA (involved in ketogenesis) is up by about 20% in response to the diet in the current study. In normal liver on a WD, up-regulation of HMGS2 is needed to prevent the build-up of acetyl-CoA and excessive mitochondria protein acetylation.[28,29] In *Atp7b*$^{-/-}$ mice, the glucose uptake and gluconeogenesis are lower, and in this case, up-regulation of mitochondrial HMG-CoA synthase may provide additional source of energy through ketogenesis and thus compensate for the energy loss due to impaired glucogenesis. Hence, shutting down cholesterol metabolism and redirecting acetyl-CoA to mitochondria may have a possible protective effect in both NAFLD and WND. However, over time, WD triggers steatosis in *Atp7b*$^{-/-}$ mice as it does in NAFLD. Thus, a delicate balance exists between compensating for energy deficits and a negative impact of fat overload, which makes WND patients vulnerable to the development of liver steatosis. Liver steatosis is a common feature of WND, and yet it does not appear in every patient. Genetic factors that dysregulate hepatic triglyceride metabolism, such as PNPLA3 mutations, which are common in NAFLD,[30] have also been found in WND patients.[17,31]

NAFL/non-alcoholic steatohepatitis is associated with copper deficiency.[32–34] A decreased hepatic copper was observed in response to WD in both mouse strains. This is likely caused by increased expression of the copper exporter ATP7A (Wooton-Kee et al,[3] Stättermayer et al,[17] and this study). Steatosis develops in spite of copper being much higher in the ko_WD mice compared with the wt mice. Furthermore, mice with ATP7B inactivated only in hepatocytes have high copper and over time develop steatosis even on NC.[12] Clearly, the effect of copper on steatosis is complex. This study, in combination with previous findings, suggests that copper misbalance seems to facilitate steatosis when inflammatory response is absent or muted. It remains to be established whether WD decreases inflammatory response in ko livers via metabolic changes or by significantly reducing copper levels in nonparenchymal cells. In addition, expression of individual proteins may contribute to the attenuating effects of copper on fatty content of the liver. For example, PCSK9, which enhances the degradation of the LDL receptor and reduces hepatic LDL uptake,[35] is down-regulated in ko_WD mice compared with wt_WD animals. It might be worth investigating whether balancing copper via its supplementation impacts inflammation development in NAFLD.

The major responses to WD were comparable between the sexes of ko animals, including reduced fat mass accumulation, the reduction of hepatic copper content, up-regulation of FasN, and the overall improvement of histology in WD groups. There were also some sex-specific differences. Male ko mice had more abdominal and inguinal fat, whereas females had stronger Oil Red O staining in the liver. The ko females showed no significant increase in glucose, whereas males did, and opposite changes in some protein expression (eg, for SCD1) were seen. The differences in ALT values suggest that liver function is more significantly improved in ko males. These differences notwithstanding, the overall impact of WD on *Atp7b*$^{-/-}$ females and males was similar.

In summary, this study provides new information on the role of copper in liver steatosis, especially in WND. These data suggest an overlap between the metabolic effects of copper overload and a high-calorie diet, which leads to their counterbalancing effects, up to a point. This delicate balance is easily disturbed by nutrient misbalance leading to steatosis development or potentially increased inflammatory response.

Acknowledgments

We thank the Hopkins Digestive Diseases Basic and Translational Research Core Center grant P30 DK089502 (NIH/NIDDK) for making the proteomics analysis possible.

Supplemental Data

Supplemental material for this article can be found at *http://doi.org/10.1016/j.ajpath.2021.09.010*.

Author Contributions

Study concept and design: A.G., S.L.; acquisition of data: A.G., S.D., L.D.; analysis and interpretation of data: A.G., S.D., K.L.G., S.L.; drafting of the manuscript: A.G.; critical revision of the manuscript for important intellectual content: A.G., S.D., L.D., R.N.C., J.P.H., S.L.; statistical analysis: A.G., study supervision: S.L.

References

1. Członkowska A, Litwin T, Dusek P, Ferenci P, Lutsenko S, Medici V, Rybakowski JK, Weiss KH, Schilsky ML: Wilson disease. Nat Rev Dis Primers 2018, 4:21
2. Huster D, Finegold MJ, Morgan CT, Burkhead JL, Nixon R, Vanderwerf SM, Gilliam CT, Lutsenko S: Consequences of copper accumulation in the livers of the Atp7b-/- (Wilson disease gene) knockout mice. Am J Pathol 2006, 168:423–434
3. Wooton-Kee CR, Robertson M, Zhou Y, Dong B, Sun Z, Kim KH, Liu H, Xu Y, Putluri N, Saha P, Coarfa C, Moore DD: Nuotio-Antar

AM: metabolic dysregulation in the Atp7b-/- Wilson's disease mouse model. Proc Natl Acad Sci U S A 2020, 117:2076–2083
4. Antonucci L, Porcu C, Iannucci G, Balsano C, Barbaro B: Non-alcoholic fatty liver disease and nutritional implications: special focus on copper. Nutrients 2017, 9:1137
5. Liggi M, Murgia D, Civolani A, Demelia E, Sorbello O, Demelia L: The relationship between copper and steatosis in Wilson's disease. Clin Res Hepatol Gastroenterol 2013, 37:36–40
6. Baranovsky AY, Belodedova AS, Fedorova TF, Palgova LK, Raikhelson KL, Kondrashina EA, Grigoreva EY: Evaluating the efficacy of diet therapy with protein component modification at Wilson disease. Voprosy Pitaniia 2020, 89:97–105
7. Einer C, Leitzinger C, Lichtmannegger J, Eberhagen C, Rieder T, Borchard S, Wimmer R, Denk G, Popper B, Neff F, Polishchuk EV, Polishchuk RS, Hauck SM, Toerne Cvon, Müller J-C, Karst U, Baral BS, DiSpirito AA, Kremer AE, Semrau J, Weiss KH, Hohenester S, Zischka H: A high-calorie diet aggravates mitochondrial dysfunction and triggers severe liver damage in Wilson disease rats. Cell Mol Gastroenterol Hepatol 2019, 7:571–596
8. Mahmood S, Inada N, Izumi A, Kawanaka M, Kobashi H, Yamada G: Wilson's disease masquerading as nonalcoholic steatohepatitis. N Am J Med Sci 2009, 1:74–76
9. Seishima J, Sakai Y, Kitahara N, Kitamura K, Arai K, Kagaya T, Yamashita T, Mizukoshi E, Honda M, Kaneko S: [A case of Wilson's disease in an elderly patient initially diagnosed with NASH]. Japanese. Nihon Shokakibyo Gakkai Zasshi 2015, 112:317–324
10. Ibrahim SH, Hirsova P, Malhi H, Gores GJ: Animal models of nonalcoholic steatohepatitis: eat, delete, and inflame. Dig Dis Sci 2016, 61:1325–1336
11. Huster D, Purnat TD, Burkhead JL, Ralle M, Fiehn O, Stuckert F, Olson NE, Teupser D, Lutsenko S: High copper selectively alters lipid metabolism and cell cycle machinery in the mouse model of Wilson disease. J Biol Chem 2007, 282:8343–8355
12. Muchenditsi A, Yang H, Hamilton JP, Koganti L, Housseau F, Aronov L, Fan H, Pierson H, Bhattacharjee A, Murphy R, Sears C, Potter J, Wooton-Kee CR, Lutsenko S: Targeted inactivation of copper transporter Atp7b in hepatocytes causes liver steatosis and obesity in mice. Am J Physiol Gastrointest Liver Physiol 2017, 313:G39–G49
13. Muchenditsi A, Talbot CC, Gottlieb A, Yang H, Kang B, Boronina T, Cole R, Wang L, Dev S, Hamilton JP, Lutsenko S: Systemic deletion of Atp7b modifies the hepatocytes' response to copper overload in the mouse models of Wilson disease. Sci Rep 2021, 11:5659
14. Aigner E, Strasser M, Haufe H, Sonnweber T, Hohla F, Stadlmayr A, Solioz M, Tilg H, Patsch W, Weiss G, Stickel F, Datz C: A role for low hepatic copper concentrations in nonalcoholic fatty liver disease. Am J Gastroenterol 2010, 105:1978–1985
15. Nobili V, Siotto M, Bedogni G, Ravà L, Pietrobattista A, Panera N, Alisi A, Squitti R: Levels of serum ceruloplasmin associate with pediatric nonalcoholic fatty liver disease. J Pediatr Gastroenterol Nutr 2013, 56:370–375
16. Nobili V, Svegliati-Baroni G, Alisi A, Miele L, Valenti L, Vajro P: A 360-degree overview of paediatric NAFLD: recent insights. J Hepatol 2013, 58:1218–1229
17. Stättermayer AF, Traussnigg S, Dienes H-P, Aigner E, Stauber R, Lackner K, Hofer H, Stift J, Wrba F, Stadlmayr A, Datz C, Strasser M, Maieron A, Trauner M, Ferenci P: Hepatic steatosis in Wilson disease–role of copper and PNPLA3 mutations. J Hepatol 2015, 63:156–163
18. Beaven SW, Tontonoz P: Nuclear receptors in lipid metabolism: targeting the heart of dyslipidemia. Annu Rev Med 2006, 57:313–329
19. Hamilton JP, Koganti L, Muchenditsi A, Pendyala VS, Huso D, Hankin J, Murphy RC, Huster D, Merle U, Mangels C, Yang N, Potter JJ, Mezey E, Lutsenko S: Activation of liver X receptor/retinoid X receptor pathway ameliorates liver disease in Atp7B(-/-) (Wilson disease) mice. Hepatology 2016, 63:1828–1841
20. Danielson PB: The cytochrome P450 superfamily: biochemistry, evolution and drug metabolism in humans. Curr Drug Metab 2002, 3:561–597
21. Ng VY, Huang Y, Reddy LM, Falck JR, Lin ET, Kroetz DL: Cytochrome P450 eicosanoids are activators of peroxisome proliferator-activated receptor alpha. Drug Metab Dispos 2007, 35:1126–1134
22. Enjoji M, Yasutake K, Kohjima M, Nakamuta M: Nutrition and nonalcoholic fatty liver disease: the significance of cholesterol. Int J Hepatol 2012, 2012:925807
23. Arguello G, Balboa E, Arrese M, Zanlungo S: Recent insights on the role of cholesterol in non-alcoholic fatty liver disease. Biochim Biophys Acta 2015, 1852:1765–1778
24. Wooton-Kee CR, Jain AK, Wagner M, Grusak MA, Finegold MJ, Lutsenko S, Moore DD: Elevated copper impairs hepatic nuclear receptor function in Wilson's disease. J Clin Invest 2015, 125:3449–3460
25. Trefts E, Hughey CC, Lantier L, Lark DS, Boyd KL, Pozzi A, Zent R, Wasserman DH: Energy metabolism couples hepatocyte integrin-linked kinase to liver glucoregulation and postabsorptive responses of mice in an age-dependent manner. Am J Physiol Endocrinol Metab 2019, 316:E1118–E1135
26. Laudanna C, Kim JY, Constantin G, Butcher E: Rapid leukocyte integrin activation by chemokines. Immunol Rev 2002, 186:37–46
27. Hogg N, Henderson R, Leitinger B, McDowall A, Porter J, Stanley P: Mechanisms contributing to the activity of integrins on leukocytes. Immunol Rev 2002, 186:164–171
28. Gusdon AM, Song K-X, Qu S: Nonalcoholic fatty liver disease: pathogenesis and therapeutics from a mitochondria-centric perspective. Oxid Med Cell Longev 2014, 2014:637027
29. Shi L, Tu BP: Acetyl-CoA and the regulation of metabolism: mechanisms and consequences. Curr Opin Cell Biol 2015, 33:125–131
30. Romeo S, Kozlitina J, Xing C, Pertsemlidis A, Cox D, Pennacchio LA, Boerwinkle E, Cohen JC, Hobbs HH: Genetic variation in PNPLA3 confers susceptibility to nonalcoholic fatty liver disease. Nat Genet 2008, 40:1461–1465
31. Ranucci G, Zuin M, Zampino R, Matarazzo M, Ferrari F, Russo MC, Miraglia Del Giudice E, Iorio R: Role of PNPLA3 polymorphism in Wilson disease: what role in metabolic syndrome and neurologic phenotype? Dig Liver Dis 2016, 48:e257
32. Burkhead JL, Lutsenko S: The role of copper as a modifier of lipid metabolism. Lipid Metabolism. Edited by Valenzuela Baez R, London, UK: IntechOpen. doi:10.5772/51819
33. Ibdah JA, Perlegas P, Zhao Y, Angdisen J, Borgerink H, Shadoan MK, Wagner JD, Matern D, Rinaldo P, Cline JM: Mice heterozygous for a defect in mitochondrial trifunctional protein develop hepatic steatosis and insulin resistance. Gastroenterology 2005, 128:1381–1390
34. Tosco A, Fontanella B, Danise R, Cicatiello L, Grober OMV, Ravo M, Weisz A, Marzullo L: Molecular bases of copper and iron deficiency-associated dyslipidemia: a microarray analysis of the rat intestinal transcriptome. Genes Nutr 2010, 5:1–8
35. Schulz R, Schlüter K-D, Laufs U: Molecular and cellular function of the proprotein convertase subtilisin/kexin type 9 (PCSK9). Basic Res Cardiol 2015, 110:4